

Diverse spatiotemporal dynamics in primate motor cortex local field potentials

Michael Rule¹, Carlos Vargas-Irwin¹, John Donoghue^{1,2}, Wilson Truccolo^{1,2}

¹Department of Neuroscience, Brown University, Providence, RI, 02912 ²U.S. Department of Veterans Affairs, Center for Neurorestoration and Neurotechnology, Providence, RI, 02912



1. Introduction

In motor cortex, β (~ 20 Hz) oscillations are elevated during movement preparation and isometric force tasks, and suppressed around movement onset. Previous studies (Rubino et al. 2009, Takahashi et al. 2015) have focused on β oscillations that appear as planar traveling waves. Understanding the mechanisms underlying modulation of β spatiotemporal patterns may clarify the functional roles of these oscillations, with potential implications for disorders in which β activity is dysregulated (e.g. Parkinson's disease). We survey motor cortex β spatiotemporal local field potential (LFP) patterns using multielectrode arrays (MEAs) in *m. mulatta* during a cued reaching and grasping task with instructed delay, and contrast these patterns to gamma (~ 50 Hz, ~ 100 Hz) spatiotemporal patterns induced by optogenetic stimulation.

2. Recording and task

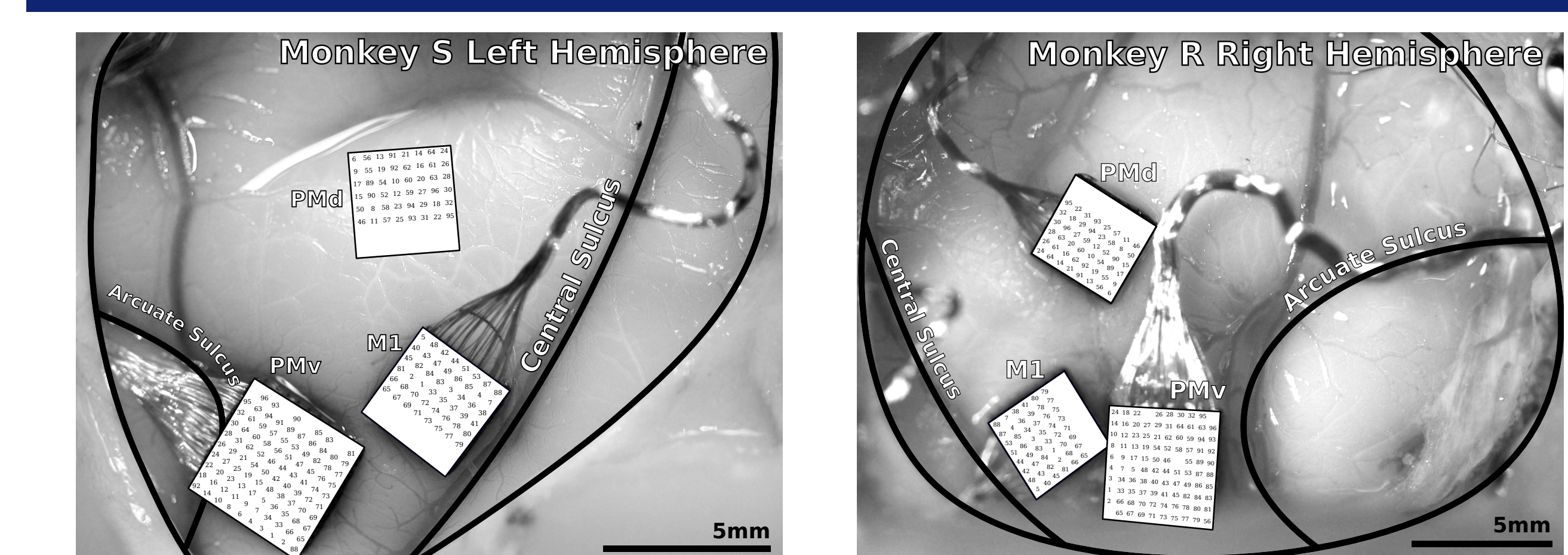


Figure 1. LFP data were recorded on 10x10 (ventral premotor cortex PMv) and 6x8 Blackrock (dorsal premotor cortex PMd and primary motor cortex M1) arrays with 0.4 mm electrode spacing. Data from two monkeys (R and S) were analyzed. Broadband (0.3 Hz - 7.5 kHz) LFPs recorded at 30 kilosamples/s were downsampled (zero-phase 4th order Butterworth, ≤ 250 Hz) to 1 kilosample/s for analysis.

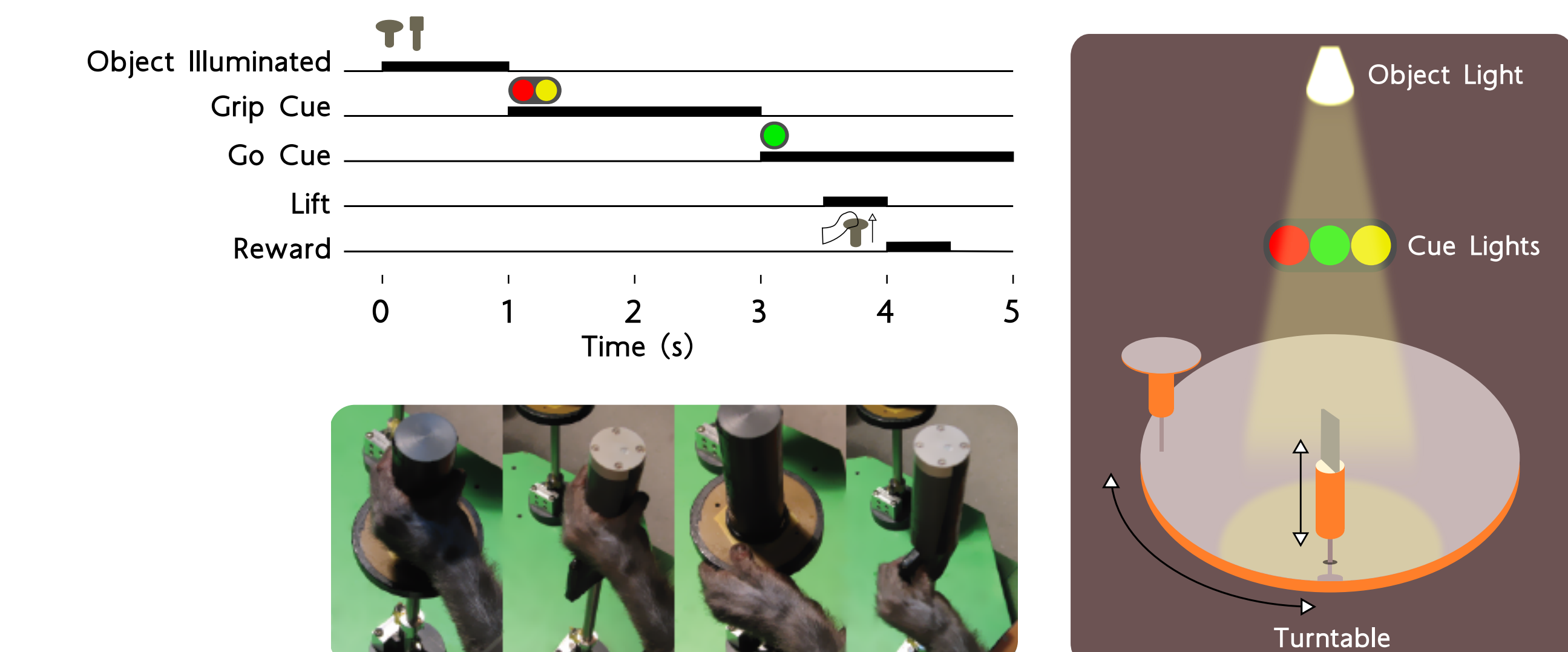


Figure 2. The Cued Grasp with Instructed Delay (CGID) task investigates sensory integration and planning of upcoming reach and grasp movements across instructed delays. When the task begins, one of two objects is presented. One second later, a cue light instructs the monkey to use either a power (left panels in the photo inset) or precision (right panels) grip to lift the object. A two second planning period follows, after which a 'Go' cue signals that the monkey may reach and grasp the object. The planning and delay periods reliably elicit β oscillations. Touch sensors detect when the monkey begins to move, and β is suppressed during a peri-movement period ± 250 ms around movement initiation.

3. Signal processing

Peaks in the beta frequency band were identified from the first second of the CGID task using multitaper spectra averaged over channels and trials. Monkey S exhibited a single β peak at 20 Hz across sessions and areas. Monkey R displayed two peaks at 17 and 26 Hz. We restrict our analysis to the lower frequency, which exhibited greater spatial synchrony. A 5 Hz band surrounding the identified β peak was extracted using a 4th order Butterworth band-pass filter applied forwards and backwards. Instantaneous phase and amplitude were extracted using the Hilbert transform.

4. Diverse beta wave patterns

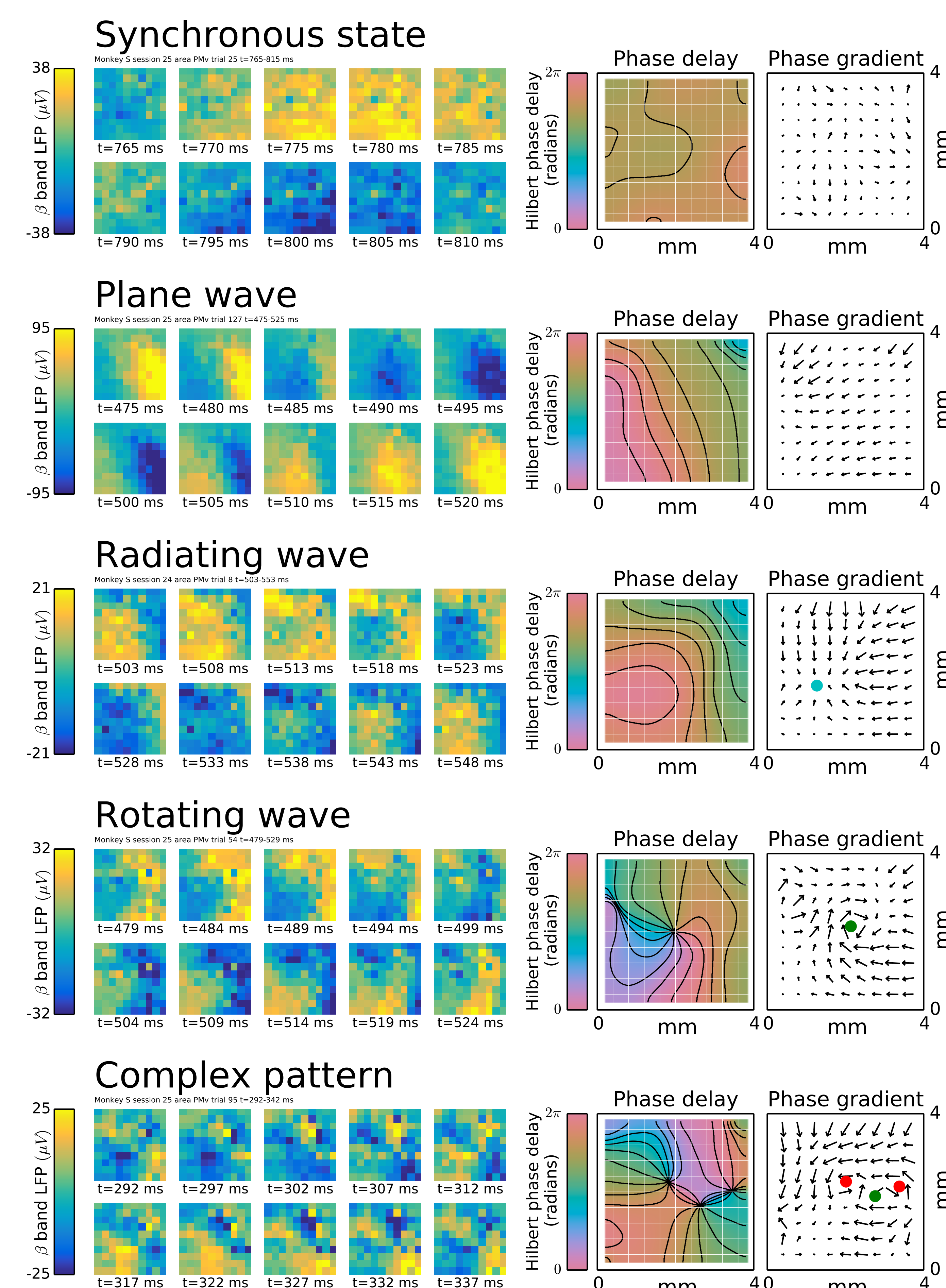


Figure 3. In addition to traveling plane waves, we see synchronous states, radiating and rotating waves, and complex patterns. Average phase delay maps were computed by unwrapping Hilbert phases at the frequency of the wave event before computing the circular mean and smoothing. Phase gradients were computed as the derivative of the average phase delay map. Missing electrodes were interpolated from nearest neighbours.

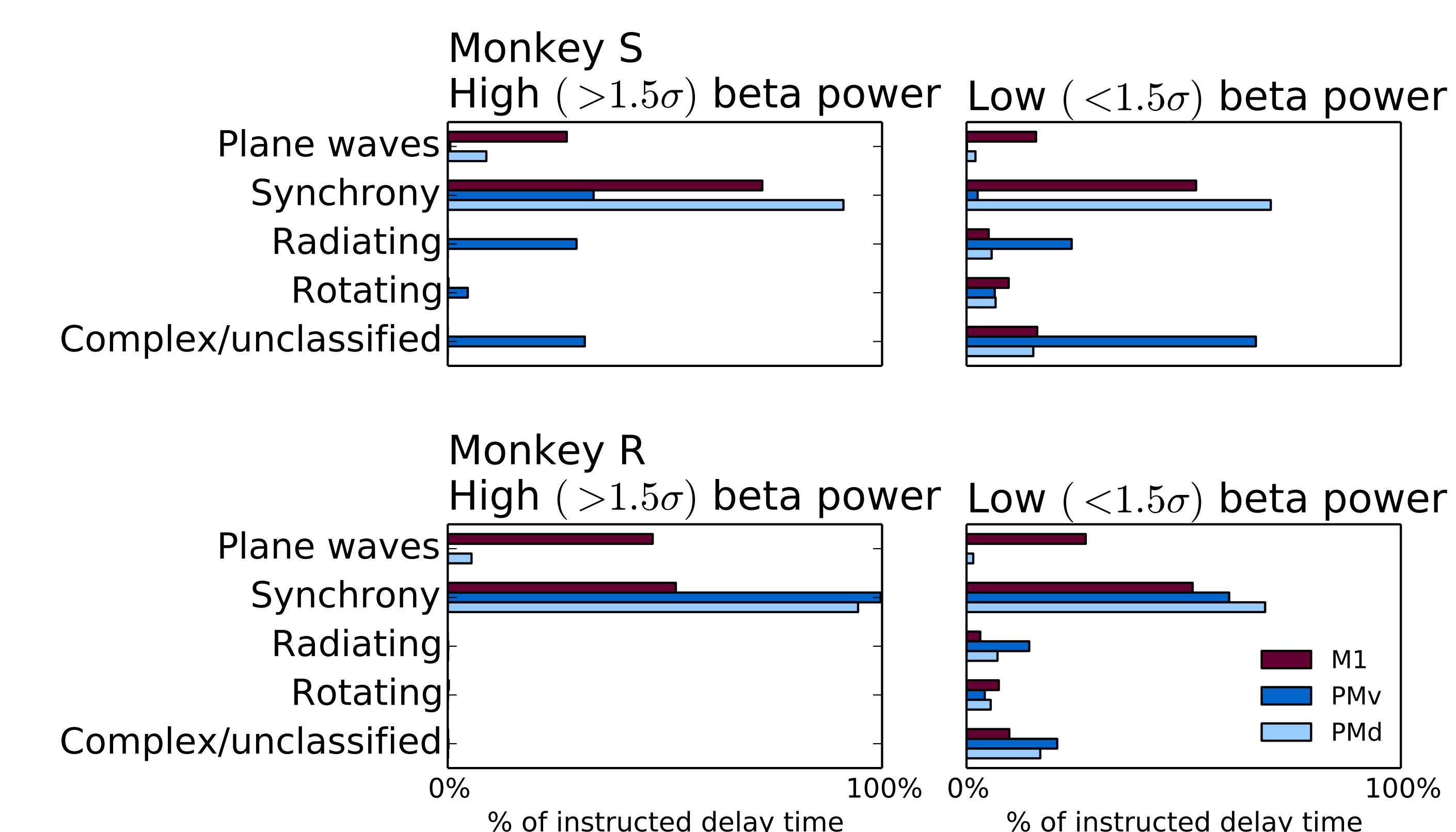


Figure 4. Wave activity patterns are diverse during the steady movement preparation period (1 s before object presentation) as shown by the summary bar plots. Time-points are separated into high and low β power by thresholding the instantaneous amplitude, with amplitudes larger than $1.5 \times$ the standard deviation of the beta signal being classified as high β power. High power is associated with synchrony or plane waves. More complex wave activity tends to occur at lower power. Some motor areas show little traveling plane wave activity, even at high beta power (Monkey S area PMd, Monkey R area PMv).

5. Classification of beta spatiotemporal activity

Wave properties were summarized using circular statistics. Spatial synchrony was summarized by the (circular) standard deviation of Hilbert phase σ_ϕ over the array. The extent to which the activity resembles a plane wave is summarized by the standard deviation of the direction of the gradient of the Hilbert phase $\sigma_{\nabla\phi}$. Waves not classified as plane waves were classified as synchronous if $\sigma_\phi < \pi/4$, such that approximately 95% of phase vectors fall within $\pi/2$ radians of each-other. Plane waves were categorized as those states for which $\sigma_{\nabla\phi} < \pi/4$.

Waves not classified as synchronous or plane waves were classified based on critical points in the gradient of the β LFP phase. Waves were classified as either containing a rotating or radiating wave, or being complex if they contained multiple critical points. Critical points were determined on a smoothed (wavelength ≥ 2 mm) estimate of the gradient of the Hilbert phase.

6. Beta wave statistics vary with amplitude

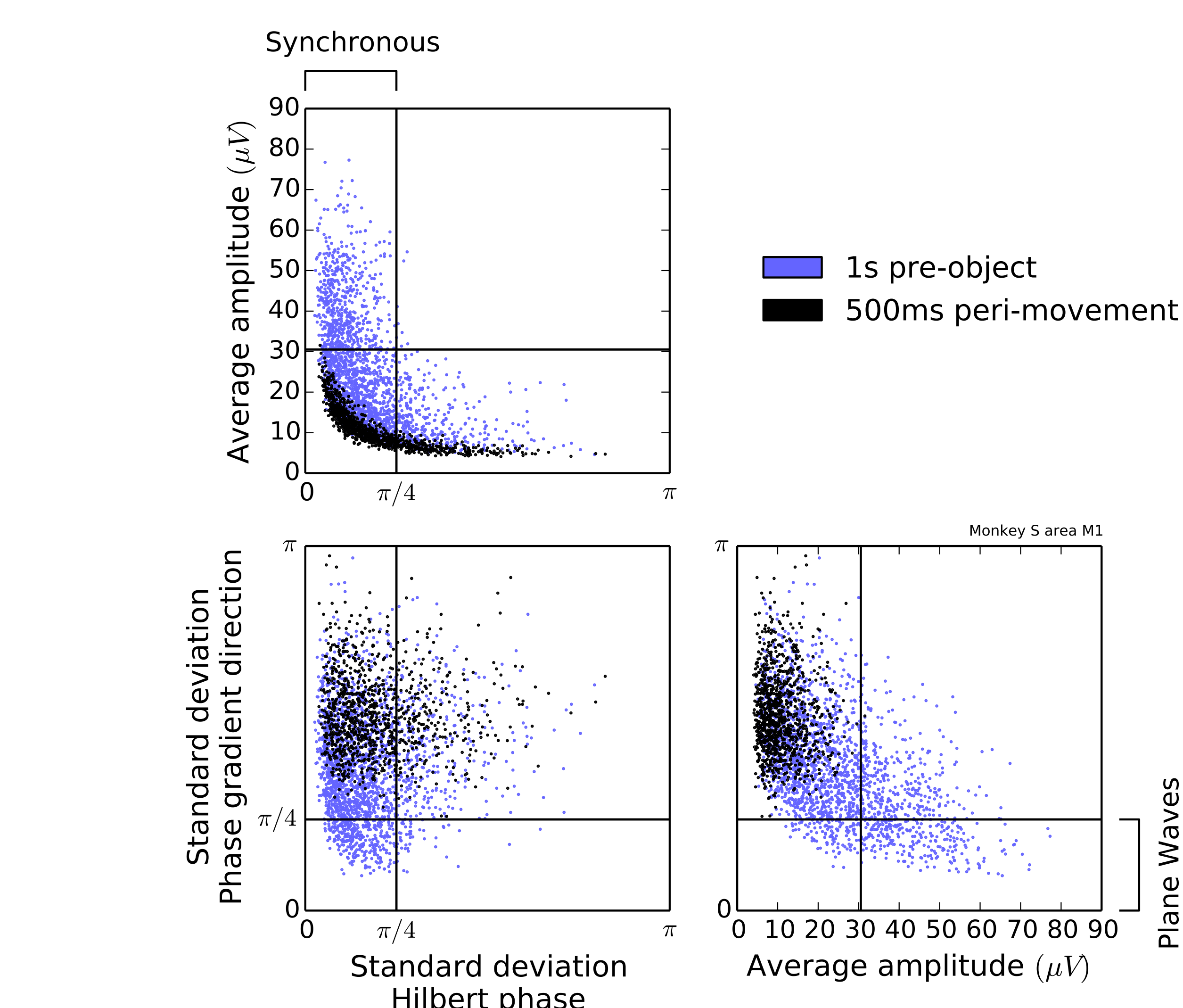


Figure 5. A comparison of β spatiotemporal statistics in monkey S area M1. Higher beta power is associated with increased synchrony and also increased tendency toward plane waves. Wave statistics are taken every 50 ms from the first second of the CGID task. Beta spatiotemporal statistics vary continuously and no clear boundaries exist separating plane wave states and synchronized states from more complex wave activity.

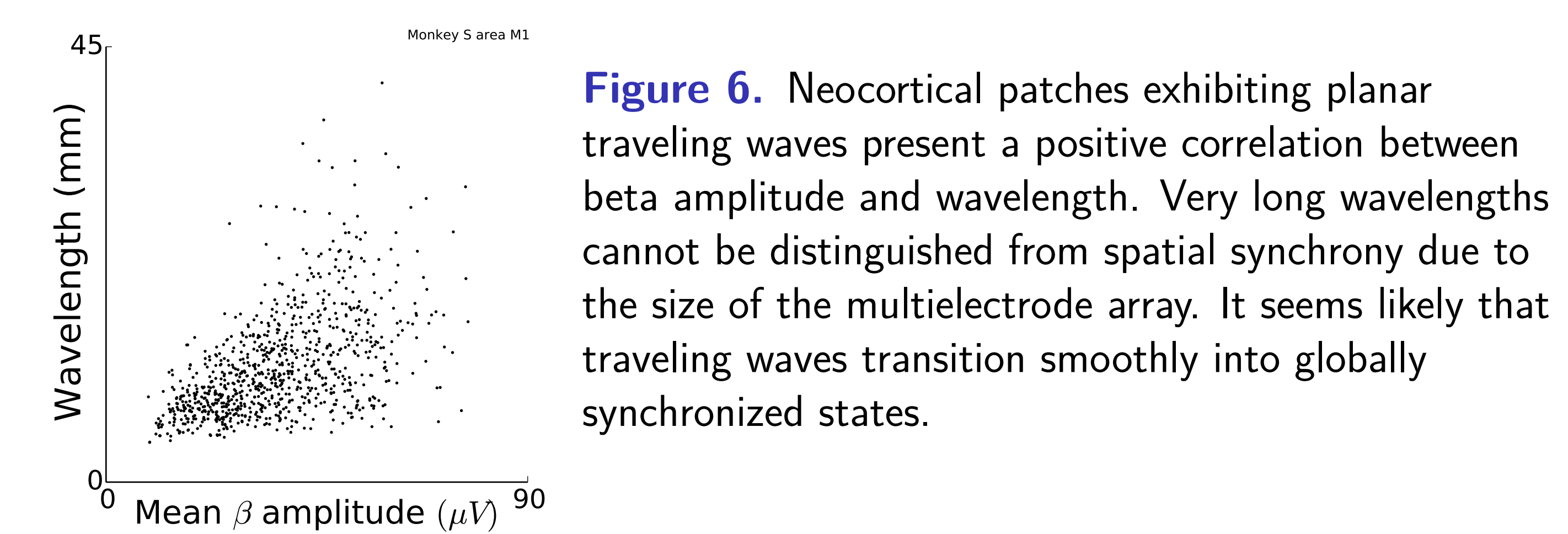


Figure 6. Neocortical patches exhibiting planar traveling waves present a positive correlation between beta amplitude and wavelength. Very long wavelengths cannot be distinguished from spatial synchrony due to the size of the multielectrode array. It seems likely that traveling waves transition smoothly into globally synchronized states.

Acknowledgements

This work is supported by the National Science Foundation Graduate Research Fellowship grant No. NSF 11-582, as well as grants NIH-NINDS R01NS079533 (WT), NIH-NINDS K01 Career Award (WT), DARPA-REPAIR (JPD; WT), NIH/NINDS NS25074 (PI: JPD; WT; co-investigator), the June Rockwell Levy Foundation and the Pablo J. Salame '88 Goldman Sachs endowed assistant professorship of Computational Neuroscience (WT).

7. Comparison to optogenetically-induced gamma

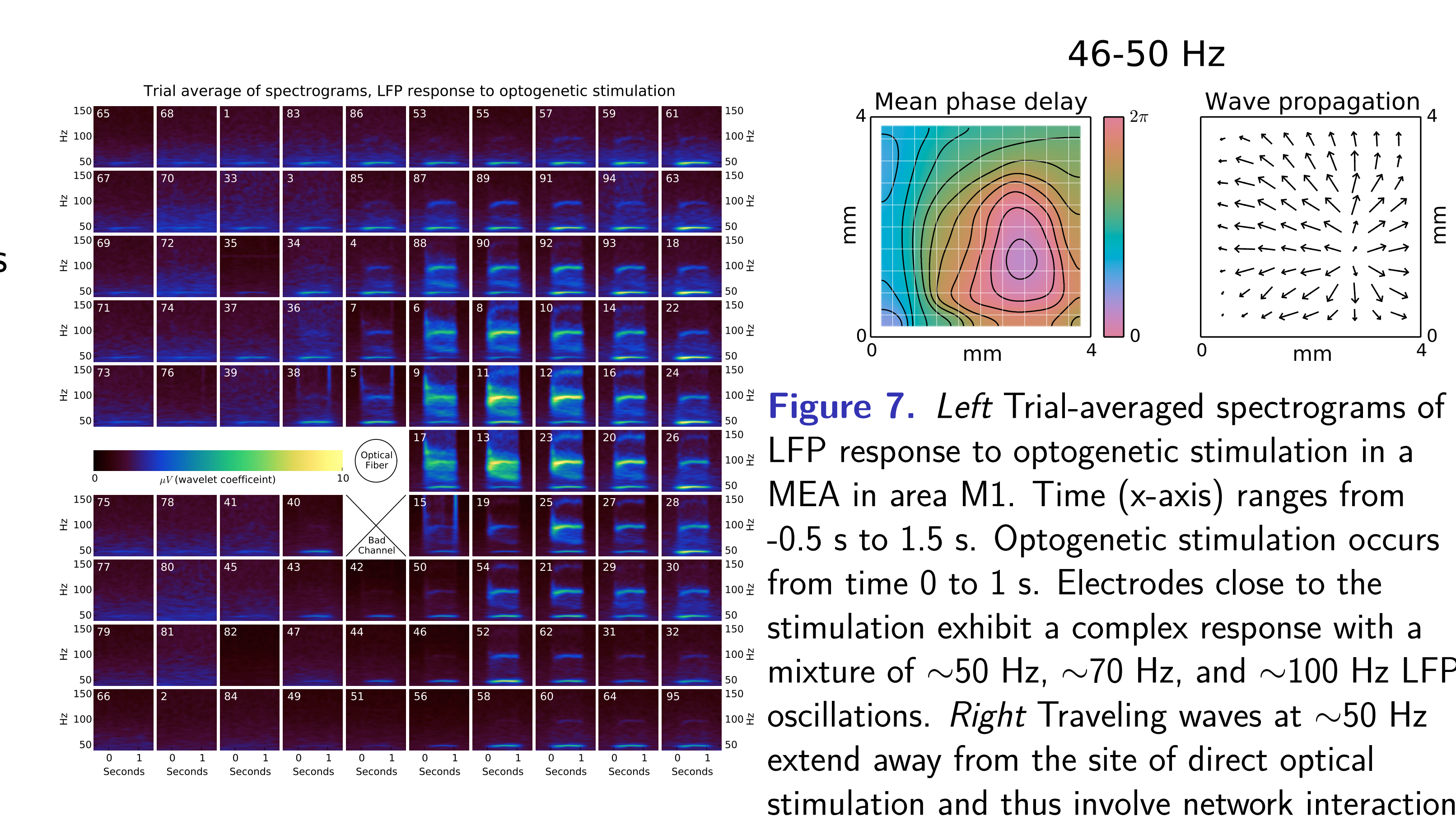


Figure 7. Left Trial-averaged spectrograms of LFP response to optogenetic stimulation in a MEA in area M1. Time (x-axis) ranges from -0.5 s to 1.5 s. Optogenetic stimulation occurs from time 0 to 1 s. Electrodes close to the stimulation exhibit a complex response with a mixture of ~ 50 Hz, ~ 70 Hz, and ~ 100 Hz LFP oscillations. Right Traveling waves at ~ 50 Hz extend away from the site of direct optical stimulation and thus involve network interactions.

8. 50 Hz gamma oscillations exhibit 2-4 mm waves

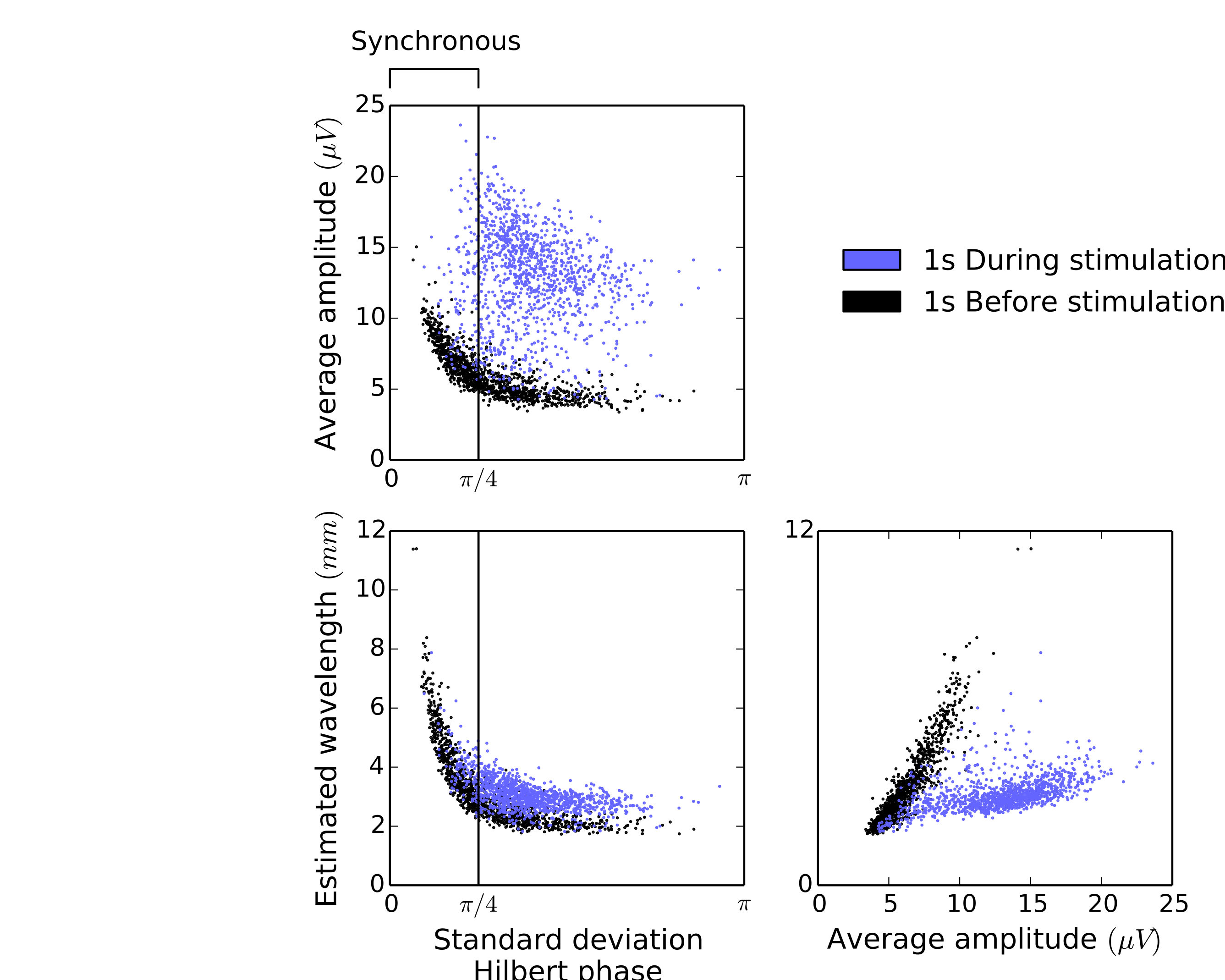


Figure 8. During optogenetic stimulation, ~ 50 Hz gamma activity exhibits a characteristic 2-4 mm wavelength and increases in amplitude as compared to the background activity. The induced oscillations lack zero-lag spatial synchrony.

9. Discussion

- Even during steady movement preparation periods, beta activity in motor cortex exhibits a variety of spatiotemporal patterns: synchronized states, plane waves, rotating and radiating waves, and complex states.
- The degree of synchrony and the spatial scale of beta spatiotemporal activity correlate with the amplitude of beta oscillations.
- In contrast, optogenetically induced ~ 50 Hz gamma oscillations show a characteristic wavelength and exhibit reduced synchrony at high amplitude.
- We conjecture that the transitions between patterns of beta activity may result from (a) fast modulation of effective lateral connectivity, (b) changes in spatiotemporal input, or (c) stochastic transitions between states in a multi-stable system.
- We speculate that diversity in beta spatiotemporal activity may have implications for directed spiking information transfer, and that the statistical properties of beta phase spatiotemporal dynamics may be important for constraining spatially extended models of motor cortex.